

# STATUS AND RESULTS OF THE UA9 CRYSTAL COLLIMATION EXPERIMENT AT THE CERN-SPS\*

S. Montesano<sup>†</sup>, CERN, Geneva, CH and  
W. Scandale, CERN, Geneva, CH, LAL, Orsay, FR, INFN, Roma, IT  
for the UA9 Collaboration

## Abstract

The UA9 experimental setup was installed in the CERN-SPS in 2009 to investigate the feasibility of the halo collimation assisted by bent crystals. Two-millimeter-long silicon crystals, with bending angles of about 150 microrad, are tested as primary collimator instead of a standard amorphous target. Studies are performed with stored beams of protons and lead ions at 270 Z GeV. The loss profile is precisely measured in the area near the crystal-collimator setup and in the downstream high dispersion area. A strong correlation of the losses in the two regions is observed and a steady reduction of dispersive losses is recorded at the onset of the channeling process. The losses around the accelerator ring are also reduced. These observations strongly support our expectation that the coherent deflection of the beam halo by a bent crystal should enhance the collimation efficiency in hadron colliders, such as the LHC.

## INTRODUCTION

In hadron colliders, like the LHC, superconducting magnet technology allows for high-intensity beams necessary to guarantee a large discovery potential. In this situation, the halo particles surrounding the beam core may produce high-power losses. Multi-stage collimation systems are implemented to safely absorb these particles. The primary collimator is the first solid target that repeatedly intercepts the diffusive halo particles, imparting to them random angular kicks by multiple Coulomb scattering. Scattered particles are thus brought into the secondary collimators and into the absorbers. Due to the very low diffusion speed and to the very small impact parameter, halo particles have a finite probability of being back-scattered in the vacuum pipe. This process produces residual losses which are detrimental for both the accelerator and the experimental detectors. Increasing the number of collimation stages improves the collimation performance. In the four-stage LHC setup, a cleaning efficiency of 99.97% is routinely reached [1].

A bent crystal replacing the primary collimator should reduce by an order of magnitude the residual collimation leakage [2, 3]. At a precise orientation of the crystal, impinging particles are trapped between atomic planes and are coherently deflected following the curvature of the lattice (channeling). For the majority of the particles, this deflection happens during the first passage through the crys-

tal. The particles that escape deflection will cross the crystal again and will have an additional probability of being channeled and absorbed in subsequent turns. Due to this process, the impact parameter of the particles with the secondary collimators and the absorbers is considerably increased. Moreover, particles channeled among the crystal planes have fewer encounters with the nuclei of the lattice resulting in a reduced probability of nuclear interactions, of diffractive scattering and, for ion beams, of fragmentation and electromagnetic dissociation events. As a consequence, crystal-assisted collimation should enhance both global and local loss suppression.

The UA9 Collaboration started to investigate crystal collimation in 2009. The single-pass interaction of the beam with the crystal is studied in details at the CERN North Area test beam. In this facility, crystals built with different technologies are tested and characterized in order to select the most suitable ones to the collimation experiment in the CERN-SPS ring. In the SPS the prototype of a crystal-assisted collimation system is implemented. Ad hoc instrumentation is installed to evaluate its collimation capabilities, in comparison with a system based on an amorphous primary target. Using this installation, a reduction of the loss rate close to the primary target has been observed when using a crystal instead of an amorphous material, both for proton [4] and for Pb ion [5] beams. Recently the reduction of the off-momentum halo population has been estimated under the same conditions [6].

## PROTOTYPE SYSTEM IN THE CERN-SPS

The conceptual layout of the UA9 experiment installed in the straight section 5 of the SPS is shown in Fig. 1. The crystal collimation prototype system is composed by the crystal itself and by the absorber. All the remaining equipment is used to study the performance and the properties of the collimation system.

### Collimation System

The crystals used by the experiment are mounted on goniometers that allow to align their lattice planes to the incoming halo particles. Each goniometer serves a pair of crystals, installed on two supports that allow horizontal linear movements. The two supports are connected with an aluminum bar. When one of the two crystals is placed at a fixed distance from the beam, it can be rotated in an angular range of tens of mrad by applying a linear movement (1 mm range) to the second one. This rotational movement

\*Work supported by EuCARD program GA 227579, in "Collimators and Materials for high power beams" (Colmat-WP) and by LARP.

<sup>†</sup>simone.montesano@cern.ch

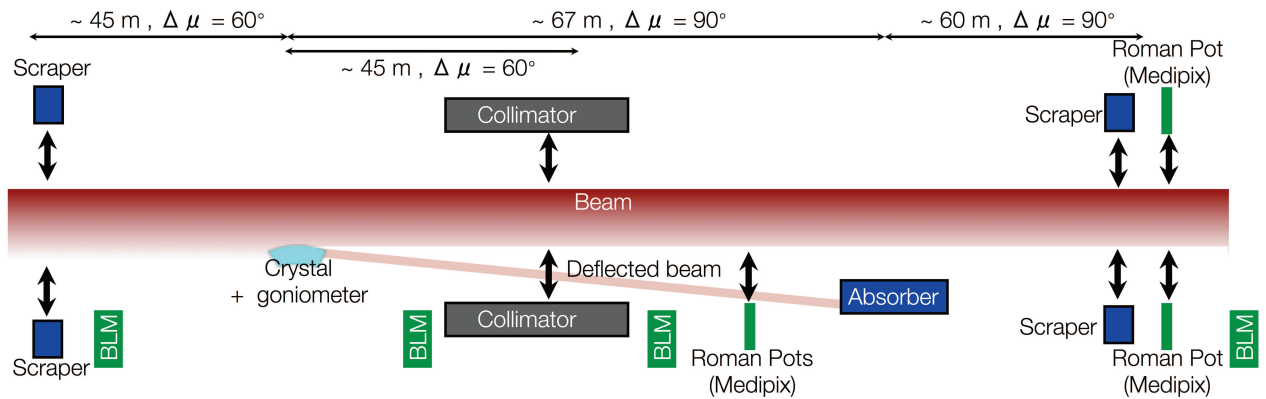


Figure 1: Conceptual layout of the UA9 experiment in the SPS.

is designed to have a resolution of  $1 \mu\text{rad}$  and an accuracy close to  $10 \mu\text{rad}$ .

The crystal used for the measurements described in this paper is a silicon strip ( $0.5 \times 70 \text{ mm}^2 \times 2 \text{ mm}$ ), with the 2 mm side in the beam direction. The holder compensates for the strip torsion down to  $0.6 \mu\text{rad/mm}$ . Torsion, bending angle ( $176 \mu\text{rad}$ ) and residual miscut ( $200 \pm 20 \mu\text{rad}$ ) of the crystal have been measured both at the test beam facility and with optical methods.

About 60 m downstream the crystals (phase advance  $\Delta\mu = 90^\circ$ ) the deflected halo is displaced by several mm with respect to the beam core and it is collected by a movable tungsten absorber. The absorber has a section of  $70 \times 60 \text{ mm}^2$  and it is 60 cm long.

### Additional Instrumentation

Between the crystal region and the absorber (42.5 m from the crystal,  $\Delta\mu = 60^\circ$ ), an LHC-type collimator with two horizontal one-meter long graphite jaws is operated. About 1.5 m and 14.5 m downstream the collimator two Roman Pot devices are installed. They comprise two horizontal motorized axes, each one supporting a secondary vacuum vessel containing a Medipix detector [7]. The pots have 0.2 mm thin aluminium walls and are 3.4 cm wide in the beam direction. The second Roman Pot also includes two vertical vessels not yet equipped with detectors.

A high dispersion region is present about 60 m ( $\Delta\mu = 90^\circ$ ) downstream the absorber. Two 10 cm tungsten scrapers are installed in this area on the two sides of the beam, as well as a third horizontal Roman Pot with Medipix detectors. The two 3 cm wide pots have 0.5 mm thick stainless steel walls.

Another two scrapers (10 cm, made of tungsten) are installed on the two sides of the beam 45 m ( $\Delta\mu = 60^\circ$ ) upstream the crystals. These devices are used to investigate the halo far away from the collimation region.

In proximity to each device, outside the vacuum pipe, different types of detectors (generically called BLM in the following) are installed: polystyrene scintillators, PEP-II-type Beam Loss Monitors, GEM detectors and LHC-type

Beam Loss Monitors [8]. They are sensitive to the production of secondary particles from inelastic interactions of the beam with the obstacles within the beam pipe. Each detector is optimized for a different range of interaction rates.

Several SPS instruments are also available but, apart from the Wire Scanner and the Beam Current Transformers (BCT), they are generally not sensitive to the relatively low current used in the experiment. Beam lifetime is monitored during data taking using BCT, Fast BCT and the Mountain Range Display. These detectors measure the intensity of the beam using electronics with different bandwidth and a comparison among them allows to estimate the fraction of de-bunched beam. Finally, the Mountain Range also computes the bunch length.

## EXPERIMENTAL RESULTS

In order to operate the crystal collimation system, its components are placed at defined distances from the beam center [9]. In particular, the crystal must be the primary target that intercepts the beam halo and the absorber the secondary one. After the setup of the collimation system, the typical procedures in use by the experiment consist in the movement of the equipment and in the observation of the induced beam loss rate variation.

The normal beam setups used for UA9 measurements include one single bunch of  $1.15 \times 10^{11}$  protons or few bunches (8 or 10) of  $1.1 \times 10^8$  fully stripped Pb ions. The beam is stored in the SPS with energy 270 Z GeV and lifetime of a few hours, depending on the selected distance of the primary target from the beam center. The average amplitude diffusion length is smaller than 0.1 nm per turn. The bunch length is few ns.

### Local Loss Reduction

Figure 2, on top, shows the loss rate measured by the BLM closer to the crystal during an angular scan of the crystal itself (black line), in the case of a proton beam. The loss rate was normalized to beam intensity and to its maximum (red line). It was then plotted as a function of the

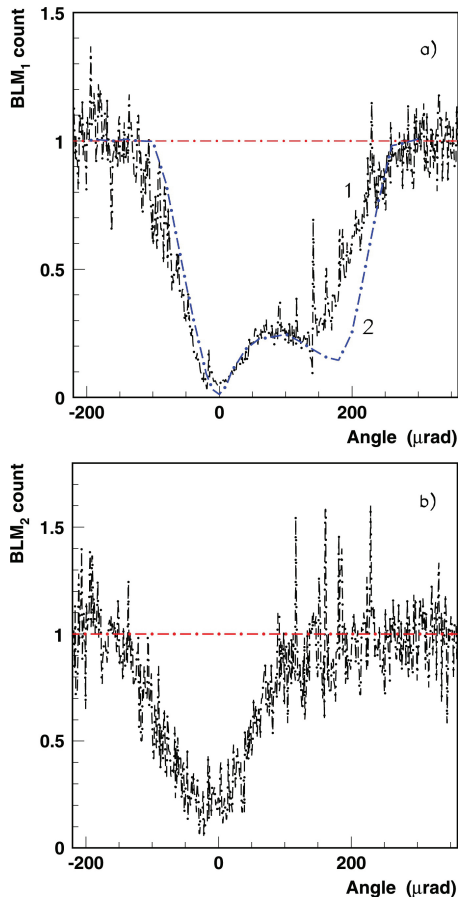


Figure 2: Beam loss rate close to the crystal (top) and in the high dispersion area (bottom) as a function of the crystal orientation, in case of a proton beam [6].

crystal orientation.

The loss rate is proportional to the number of halo particles that undergo inelastic interaction when impinging on the crystal. It shows a characteristic dependence on the crystal orientation. The rate is maximal when the crystal is behaving like an amorphous material. The minimum occurs when the fraction of particles deflected by the crystal through channeling interaction is maximal. On the right of the minimum, there is a wide angular range of significant loss reduction due to volume reflection. For this crystal orientation, particles are reflected by the curved lattice, thus reaching the absorber aperture within few passages and reducing the inelastic scattering probability.

The reduction factor is defined as the ratio between the loss rate registered when the crystal is in amorphous orientation and the one when the crystal is in channeling orientation. For a proton beam, a reduction factor between 5 and 20 is observed.

A similar measurement is shown in Fig. 3 for a Pb ion beam. The shape of the loss rate distribution as a function of crystal orientation is similar to the one observed for protons. The channeling orientation is found at the same angle. The reduction factor that is observed is smaller than

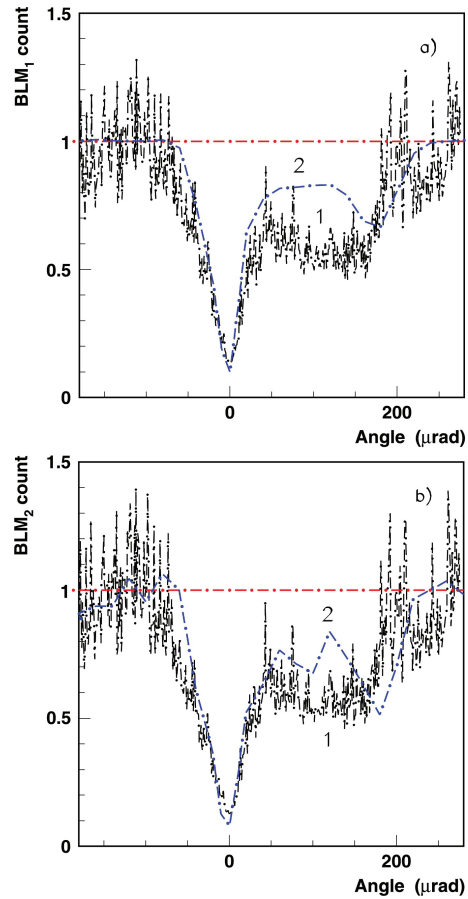


Figure 3: Beam loss rate close to the crystal (top) and in the high dispersion area (bottom) as a function of the crystal orientation, in case of a Pb ion beam [6].

for protons, within 3 and 7. This difference is expected considering that the cross section of Pb ion beam attenuation in the crystal is about 10 times larger than for protons [6].

In both figures, a blue line corresponding to the simulated results is shown. The simulation predicts the shape of the distribution with some small discordance, mainly in the volume reflection interval.

During the operation of the collimation system, the crystal orientation with respect to the beam should be fixed within the critical angle ( $\sim 13 \mu\text{rad}$  for 270 GeV/c protons) to maximize the probability of channeling interactions. By comparison with the simulation, it is proven that the observation of the loss rate is the optimal procedure to find the best orientation for the crystal.

### Estimation of Collimation Efficiency

The efficiency of the crystal collimation system is defined as the ratio between the number of particles deflected to the absorber and the total number of particles impinging on the crystal.

In order to estimate the efficiency, the collimator internal jaw is moved towards the beam after setting up the crystal collimation system. The loss rate provoked by the move-

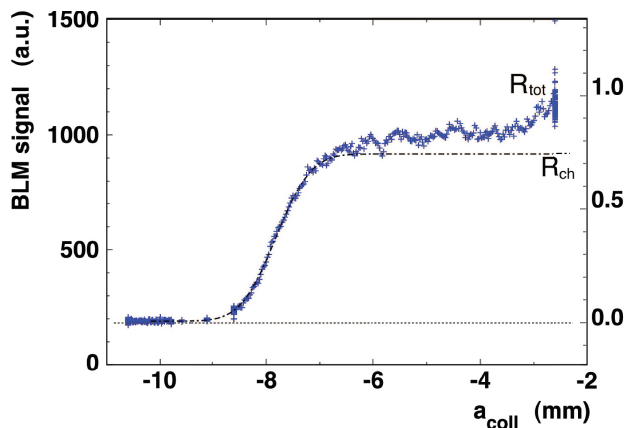


Figure 4: Dependence of the loss rate on the collimator jaw position during the measurement of the crystal collimation efficiency [4].

ment of the jaw is showed in Fig. 4 for a proton beam with energy 120 GeV/c and a different crystal [4]. It is assumed that this loss rate is proportional to the number of particles impinging on the collimator jaw.

During the movement the deflected beam is intercepted, increasing the local loss rate to a value  $R_{ch}$ . When the jaw finally touches the beam core a loss rate  $R_{tot}$  is measured. Assuming that the number of particles impinging on the primary aperture restriction is constant, the efficiency is estimated from the ratio  $R_{ch}/R_{tot}$  [10].

Using this method, the efficiency was estimated for several beam conditions and crystals. The efficiency for protons beams has been found between 70 and 80%, while the one for Pb ion beams between 50 and 70%.

If one of the Roman Pots is inserted between the crystal and the absorber, the deflected beam traversing the Medipix detector can be studied (see Fig. 5). Careful positioning is necessary, in order to avoid touching the beam core with the Roman Pot vessel. The distance of the deflected beam from the beam core and its width can be fit from the spatial distribution measured by the Medipix. From comparison with simulated data, the exact orientation of the crystal and the efficiency of the channeling process can be estimated [4].

### Leakage from the Collimation System

In order to measure the fraction of particles escaping from the collimation area, the scrapers installed in the high dispersion region and upstream the crystal are used.

In the high dispersion region, particles that have lost energy experience a larger lateral displacement. Therefore it is interesting to investigate the effect of crystal collimation on this off-momentum halo. By moving the scraper towards the beam the loss rate in this area can be artificially increased, in order to obtain a signal on the BLM proportional to the halo population. It is however necessary to keep the scraper far enough from the primary beam, in order not to perturb the collimation system.

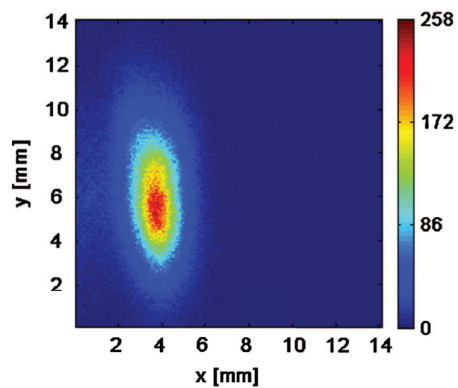


Figure 5: The image of the deflected beam, obtained with a Medipix detector [4].

Figures 2 and 3, on the bottom, show the loss rate measured in the dispersive area during an angular scan for a proton and a Pb ion beam respectively. By comparison with the top part of the figures it is observed that the loss rates in the high dispersion region are well correlated with the loss rates recorded close to the crystal. In particular the minimum of the distribution occurs in both cases for the channeling orientation of the crystal. A reduction factor for the off-momentum halo population can be defined as the ratio between the loss rate in amorphous orientation and the one in channeling orientation. The measured reduction factor for proton beams is between 2 and 6, generally lower than the one measured at the crystal. For Pb ion beams, the reduction factor in the dispersive area is equal to the one at the crystal (between 3 and 7).

### Loss Map in the SPS Ring

The loss maps allow to study the distribution of the beam losses around the entire accelerator ring. They can be used to evaluate the efficiency of a collimation system, by comparing the total number of particle lost in the machine and the number of particle lost in the collimation system.

Unfortunately, it is not easy to perform loss map measurements in the SPS. The SPS in fact is subject to very low loss rate during normal operations. The losses are concentrated in few particular regions (injection and extraction regions). The SPS beam loss monitor system (one sensor is installed close to each quadrupole) is indeed optimized for machine protection and has a limited dynamical range.

For this reasons, in order to try to measure loss maps, the intensity of the usual beam was increased to 48 bunches. Using a proton beam with total intensity  $5 \times 10^{12}$ , SPS beam loss monitor data were acquired for 10 minutes keeping the crystal in channeling orientation. The measurement was repeated after rotating the crystal to amorphous orientation. Data were normalized to beam intensity and compared. Figure 6 shows the results for the section 6 of the SPS (the first section following the UA9 installation, 1 km downstream). The losses registered with the crystal

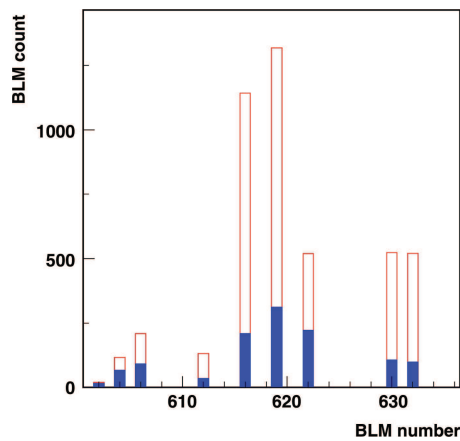


Figure 6: Loss map measured in sector 6 of the SPS with crystal in channeling (blue) and in amorphous (red) orientation [6].

in channeling orientation (blue histogram) are a few times smaller than the one measured with the crystal in amorphous orientation (red histogram).

## TOWARDS INSTALLATION IN THE LHC

Following the results obtained with the prototype system installed in the SPS, the UA9 collaboration has requested to install a system to test crystal collimation in the LHC.

Preliminary studies to define the optimal layout of the crystal collimation system have started. The minimal setup includes one single crystal and uses the already operational secondary collimators as possible absorbers. The natural place to install such a crystal is close to the primary collimators. This would allow a direct comparison of the performance of the amorphous targets with the one of the crystal. Simulations performed at injection energy (450 GeV) and with all the standard collimators in place, show that the extracted beam reaches one of the secondary horizontal collimators with impact parameter larger than 1 mm (for a deflection angle larger than  $30 \mu\text{rad}$ ). Alternative possibilities are being investigated, since the area close to the primary collimators is extremely radioactive and has tight space allowance.

In order to optimize channeling efficiency, the crystalline planes should be oriented within the critical angle with respect to the incoming halo particles. The critical angle is proportional to  $\sqrt{E}$ , where  $E$  is the energy of the particle. Therefore, a goniometer suitable for the LHC should have an accuracy better than  $2 \mu\text{rad}$ . Three developments have been started, to build such a device. An improved version of the goniometer already installed in the SPS has been prepared by collaborators in IHEP (Russia). The industrial partner CINEL has built a system whose accuracy in static regime matches the requirements. Tests are ongoing to assess its performance in the dynamic regime. Finally, a collaboration with the industrial partner ATTOCUBE has begun to develop a piezoelectric device.

Other open issues in view of a future installation in the LHC are the crystal collimation performance at high intensity and halo flux rate, as well as the robustness of the crystal and the absorber to high halo flux.

## CONCLUSION

UA9 results demonstrate that crystal collimation can be routinely achieved for proton and Pb ion beams with a robust and well-reproducible procedure. Its performance is superior to that of a standard collimation setup with amorphous primary target. When the crystal is in channeling orientation, the loss rate close to the crystal and the off-momentum halo escaping from the collimation region are strongly reduced. Encouraging yet incomplete results about loss reduction in the entire accelerator ring have been found.

Following these results, the UA9 collaboration has requested the installation of a minimal setup to test crystal collimation in the LHC. The LHC Experiments Committee has recommended the installation of such a system. The preparatory studies and R&Ds have started.

## REFERENCES

- [1] G. Valentino et al. Multi-turn losses and cleaning in 2011 and 2011. *LHC Beam Operation Workshop*, Evian, 2011.
- [2] R. W. Assmann et al. Optics study for a possible crystal-based collimation system for the LHC. *EPAC 06*, Edinburgh, 2006.
- [3] W. Scandale. Crystal-based collimation in modern hadron colliders. *CERN-2009-04*, 2008.
- [4] W. Scandale et al. First results on the sps beam collimation with bent crystals. *Physics Letters B*, 692(2):78–82, 2010.
- [5] W. Scandale et al. Comparative results on collimation of the SPS beam of protons and Pb ions with bent crystals. *Physics Letters B*, 703:547–551, 2011.
- [6] W. Scandale et al. Strong reduction of the off-momentum halo in crystal assisted collimation of the SPS beam. *Physics Letters B*, 714:231–236, 2012.
- [7] M. Campbell. 10 years of the Medipix2 collaboration. *Nucl. Instrum. Meth. A* 633 S1, 2011
- [8] W. Scandale et al. The UA9 experimental layout. *Journal of Instrumentation*, 6(10):T10002, 2011.
- [9] S. Montesano et al. Apparatus and experimental procedures to test crystal collimation. *IPAC 12*, New Orleans (USA), 2012.
- [10] V. Previtali. Performance evaluation of a crystal-enhanced collimation system for the LHC. *PhD thesis, EPFL*, 2010.